2001

Intrinsically Bent DNA in the Promoter Regions of the Yeast GAL1–10 and GAL80 Genes

Ralph C. Bash
Arizona State University at the Tempe Campus

Jeff Vargason
George Fox University, jvargason@georgefox.edu

P. Shing Ho
Oregon State University, Corvallis, OR

D. Lohr
Arizona State University at the Tempe Campus

Intrinsically Bent DNA in the Promoter Regions of the Yeast *GAL1–10* and *GAL80* Genes*

Ralph C. Bash‡, Jeffrey M. Vargason§¶, Santiago Cornejo‡, P. Shing Ho§‖, and D. Lohr‡**

From the ‡Department of Chemistry and Biochemistry, Arizona State University, Tempe, Arizona 85287-1604 and the §Department of Biochemistry and Biophysics, Oregon State University, Corvallis, Oregon 97331

Circular permutation analysis has detected fairly strong sites of intrinsic DNA bending on the promoter regions of the yeast *GAL1–10* and *GAL80* genes. These bends lie in functionally suggestive locations. On the promoter of the *GAL1–10* structural genes, strong bends bracket nucleosome B, which lies between the UAS_G and the *GAL1* TATA. These intrinsic bends could help position nucleosome B. Nucleosome B plus two other promoter nucleosomes protect the TATA and start site elements in the inactive state of expression but are completely disrupted (removed) when *GAL1–10* expression is induced. The strongest intrinsic bend (~70°) lies at the downstream edge of nucleosome B; this places it approximately 30 base pairs upstream of the *GAL1* TATA, a position that could allow it to be involved in *GAL1* activation in several ways, including the recruitment of a yeast HMG protein that is required for the normally robust level of *GAL1* expression in the induced state (Paull, T., Carey, M., and Johnson, R. (1996) *Genes Dev.* 10, 2769–2781). On the regulatory gene *GAL80*, the single bend lies in the non-nucleosomal hypersensitive region, between a *GAL80*-specific far upstream promoter element and the more gene-proximal promoter elements. *GAL80* promoter region nucleosomes contain no intrinsically bent DNA.

The bonds that form the backbone of DNA have significant rotational freedom. As a result, DNA is typically a flexible macromolecule. However, it was established some time ago that particular DNA sequences can cause a region of DNA to assume a distinct nonlinear curved structure (for reviews, see Refs. 2–5). This property is referred to as intrinsic DNA bending or DNA curvature. Intrinsically bent DNA has a preferred conformation and thus is more rigid than a typical DNA molecule, a property that causes this DNA to migrate more slowly than random (non-bent) DNA during polyacrylamide gel electrophoresis (6, 7).

Intrinsic DNA bending has been found to play a significant role in the transcriptional regulation of many prokaryotic genes (8, 9). In prokaryotes, intrinsic bending helps implement both repression and activation, operating by a number of distinct mechanisms. However, the possible role of intrinsic bending in eukaryotic transcription is less clear. Schroth *et al.* (10) described two intrinsically bent regions that flank the transcription start site of rRNA in *Physarum.* An intrinsic bend in the promoter region has been detected on several human genes: β-actin (11), β- and ϵ-globin (12), and *cdc2* (13). Intrinsic bends that are binding sites for transcription factors are found in the E2F consensus recognition site (14) and in an enhancer of the human interferon β gene (15). Of course, there are numerous examples of protein-induced DNA bending on eukaryotic promoters involving both "architectural" proteins like HMG[1] (16) and specific transcription factors (14–15, 17–20).

For a number of years, our laboratory has been studying the yeast *GAL* genes, one of the most intensely studied model systems for eukaryotic gene regulation (21–25). The structural genes, *e.g. GAL1–10,* are induced to very high level expression in galactose by the action of the activator Gal4p. Gal4p binds to activation sequences (UAS_G) that lie upstream of *GAL* genes (Fig. 1) and activates transcription in a process that depends on gene-proximal TATA elements and involves numerous coactivators and general transcription factors including TBP (for a review see Ref. 25). The activation function of Gal4p is modulated by Gal80p, an inhibitory regulator that binds specifically to the activation domain of Gal4p, thus preventing gene activation in nongalactose carbon sources (21). The gene that encodes this negative regulator is constitutively expressed at a basal level in all carbon sources via an Inr element located at +1 and at higher induced levels in galactose through a UAS_G and TATA (26, 27). Both basal and induced *GAL80* expression depend on the UAS_{GAL80} (Fig. 1), a far upstream *GAL80*-specific activation sequence (27).

During the course of working with *GAL* promoter region DNA, we have noticed gel migration anomalies. The results presented below confirm the source of these anomalies, intrinsic DNA bends on the *GAL1–10* and *GAL80* promoter DNAs. The extensive knowledge base for *GAL* regulation allows us to correlate quite accurately the locations of the intrinsic bends with the locations of known DNA regulatory sites on these promoters. In addition, the chromatin structure of both the *GAL1–10* (28) and *GAL80* promoter regions (29) are known, as well as the role that promoter nucleosome structure plays in regulation of the *GAL* genes (*cf.* Refs. 25 and 30). Thus, perhaps more importantly, we are also able to correlate bend locations with promoter nucleosome locations, a comparison that has not been possible with the intrinsic bends detected on other eukaryotic promoters. Indeed, this comparison provides some very interesting results regarding the relationship of bends and nucleosomes.

* The costs of publication of this article were defrayed in part by the payment of page charges. This article must therefore be hereby marked "*advertisement*" in accordance with 18 U.S.C. Section 1734 solely to indicate this fact.

¶ Supported by Grant MCB-9728240 from the National Science Foundation.

‖ Supported by Grant ES00210 from the National Institute of Environmental Health Sciences.

** To whom correspondence should be addressed. Tel.: 480-965-5020; Fax: 480-965-2747; E-mail: dlohr@asu.edu.

[1] The abbreviations used are: HMG, high mobility group; bp, base pairs; TBP, TATA-binding protein; UAS, upstream activation sequence.

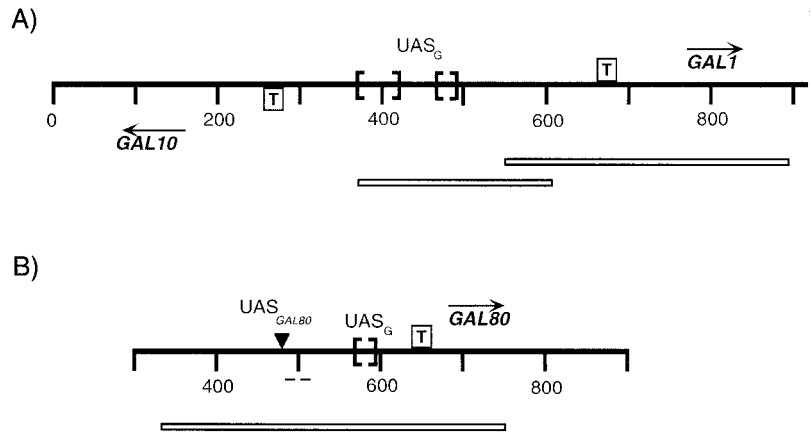

FIG. 1. **Maps of the GAL1–10 and GAL80 promoter and 5′ coding regions.** The intergenic region of *GAL1–10* (*panel A*) and the upstream region of *GAL80* (*panel B*) are shown. The *numbers below* the *thick line* are base pairs measured from a reference *Eco*RI (*GAL1–10*) or *Mbo*II site (*GAL80*). Upstream activation sequences (UAS_G) are delineated by *brackets*, TATA boxes by a *boxed T*, a *GAL80*-specific activation sequence (UAS_{GAL80}) by an *inverted triangle*, an ~20-bp purine-pyrimidine tract by a *short dashed line*, and the regions used in the cyclic permutation experiments of Figs. 4 and 5 by *rectangles*. The transcription start sites are located at the origins of the *horizontal, labeled arrows*.

EXPERIMENTAL PROCEDURES

Plasmids containing the promoter regions of *GAL1–10* or *GAL80* (29, 31) were isolated according to Birnboim (32) and the insert DNA excised from the plasmids by restriction digestion as follows: *Eco*RI to release a 907-bp fragment containing the *GAL1–10* intergenic region; *Eco*RI-*Nco*I to release a 1005-bp fragment containing the upstream and 5′ coding region of *GAL80*. The insert DNA was separated from the plasmid vectors by preparative gel electrophoresis, the bands of interest were identified by UV shadowing, and the DNA was eluted from the gel by a gel crush method (33).

Gel Mobility—Restriction digests of promoter region DNA were electrophoresed on analytical gels (7.5%, 29.4:1 acrylamide:bisacrylamide-TBE), along with DNA size standards (pBR322-*Msp*I, ϕx174-*Hae*III) at 4 °C and 1.5 V/cm for 96 h in the absence or presence of 1 μg/ml ethidium bromide in the gels (34). The relative migrations (R_f) of DNA fragments were calculated by dividing band migration distances by the migration distance of a DNA standard, which would correspond to the same number of base pairs, determined from a plot of migration distance *versus* size for standard reference digests, *e.g.* pBR-*Msp*I. This method avoids the possibility of an intrinsically bent standard DNA fragment affecting promoter R_f values.

Circular Permutation—The desired DNA fragment was cut out from the promoter region DNA by restriction digestion and isolated using polyacrylamide gel electrophoresis, UV shadowing, and gel crush as described above. To make concatamers of the fragment, a T4 ligase blunt end reaction was carried out at 16 °C for 2–6 h, and *Bam*HI linkers were then ligated to the ends of these fragments (T4 ligase, 16 °C for 16 h). The resulting products were digested with *Bam*HI and analyzed on a 1.5% agarose gel to estimate the DNA concentration. This concatamer mixture was ligated into a *Bam*HI cut (and dephosphorylated) pBSK$^+$ vector under sticky end ligation conditions (1:1–4:1 insert to plasmid molar ratio), transformed into a UV-XL1Blue *Escherichia coli* host and grown in L broth to stationary phase with ampicillin selection (35). The resulting library was screened for the desired head-to-tail dimer insert using standard α-complementation and miniprep restriction digest screening techniques (35). The desired dimeric fragments were isolated using polyacrylamide gel electrophoresis/UV shadowing/gel crush.

For the circular permutation assay, a head-to-tail dimer fragment was cut with various single cut (per monomer unit) restriction enzymes and analyzed on polyacrylamide gels (8%, 1-mm thick) run at 4 °C and 1.5 V/cm for 120–200 h. R_f values for the monomer fragments were calculated by dividing the migration distance for the fragment by the migration distance of a standard DNA fragment of the same length (obtained from a plot of log bp *versus* migration for a standard restriction digest). The bend center was determined as the intersection of two lines on the plot of restriction cut site *versus* R_f from the circular permutation analysis. Each line was a best fit of a weighted least squares formula for data approaching the maximum R_f from the left or right, respectively. Where there was a scarcity of data approaching from one side, the data were wrapped from the other side of the plot. A minimum of four independent electrophoretic determinations were carried out for each bend site.

DNA Simulations—The program LORDS (Long Range DNA Simulator, P. S. Ho laboratory), which incorporates the helical parameters of rise, twist, roll, and tilt from any number of different bending models, was used to construct low resolution, three-dimensional structures for the *GAL1–10* and *GAL80* promoter DNA (*cf.* Fig. 2). In this study, we used the parameters derived by Bolshoy *et al.* (36), the parameters derived by Goodsell and Dickerson (37), or the parameters from Brukner *et al.* (40) to construct DNA models with LORDS.

RESULTS

We initially applied several computational bending algorithms (36–38) to the promoter DNA sequences of the *GAL1–10* and *GAL80* genes. Although all models predicted intrinsic bending, the models differed in the predicted locations and strengths of the bends within the promoter regions (*cf.* Fig. 2*A*). Thus, a preliminary experimental screening method was utilized to identify intrinsically bent regions of DNA on which to carry out circular permutation analysis. The screen involved carrying out several restriction digests of *GAL1–10* and *GAL80* promoter DNA and testing the resulting sets of small (100–400-bp) fragments for anomalous migration during polyacrylamide gel electrophoresis (see "Experimental Procedures"). Two such sets of results are shown in Fig. 3.

The data identify some *GAL1–10* promoter DNA fragments that consistently demonstrate anomalously slow migration under these electrophoresis conditions. That the anomalous migration is due to intrinsic bending is confirmed by the observation that the anomalies completely disappear when electrophoresis is carried out in the presence of ethidium bromide, a treatment that has been shown to remove migration anomalies that are caused by bending (34). DNA fragments containing the region immediately upstream of the *GAL1* TATA consistently show the most anomalous migration behavior (*b* or *1*, Fig. 3*A*). However, in a fragment with an upstream terminus closer to *GAL1*, at 659 bp, the anomalous migration is largely abolished (not shown). This observation would suggest that an intrinsic DNA bend lies between 600 and 659 bp.

Based on those types of observations, we carried out a circular permutation analysis (6) on a tandem head-to-tail dimer of a fragment containing DNA from 550 to 896 bp on the *GAL1–10* promoter (Fig. 1), as described under "Experimental Procedures." In this type of analysis, the dimer is cleaved with restriction enzymes that cut once within each monomer unit, producing a set of identically sized (monomer) DNA molecules but with varying internal locations of any intrinsic bends. The fragments with the highest relative mobility arise when the restriction site that is cut lies at or near the center of the bend; monomer fragments produced by this enzyme will not contain the entire internal bend (6). The results are shown in Fig. 4. To locate the bend center, we carried out a best-fit analysis on each of the two distinct arms of the plot. By this analysis, the bend center maps to 645 bp. Again, the presence of ethidium bromide removes all anomalous migration and all R_f differences among the fragments (Fig. 4, *open circles*), indicating that intrinsic curvature is responsible for the migration anom-

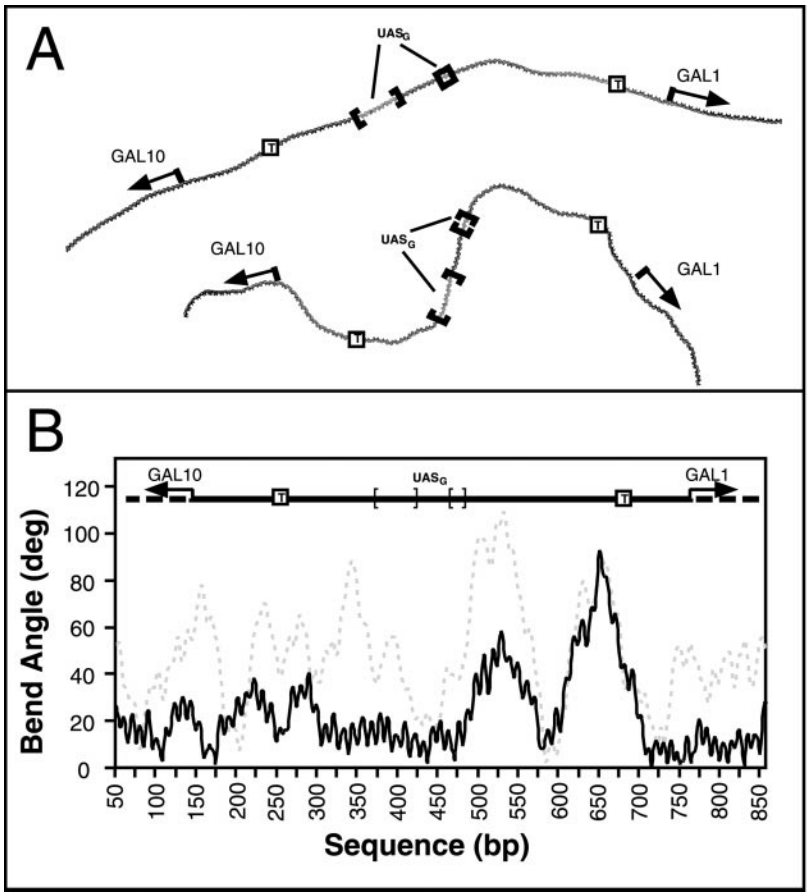

FIG. 2. **Predicted intrinsic bending in the 907-bp GAL1–10 intergenic region.** *A*, low resolution models of the yeast *GAL1–10* gene were constructed using the program LORDS (see "Experimental Procedures"). The *upper* model was constructed using the parameters of Goodsell and Dickerson (37), whereas the *lower* model used the parameters of Bolshoy, Harrington, and colloeagues (36). The UAS_G, TATA (*boxed T*) and transcription start sites are located *above* the DNA. *B*, bend angles in the *GAL-10* intergenic sequence. The degrees of bending across the intergenic region are compared for the Goodsell and Dickerson (*solid line*) and the Bolshoy and Harrington models (*dashed line*) discussed in *A*. The bp values (*x* axis) correspond to those given in Fig. 1*A*. A 100-bp window size was used in the analysis.

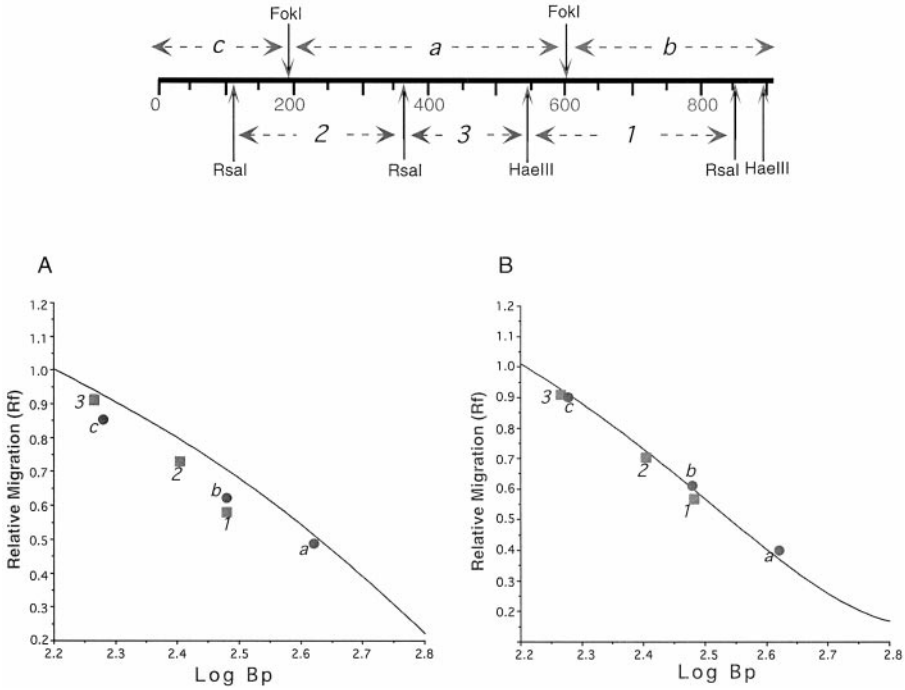

FIG. 3. **Anomalous gel mobility of GAL1–10 promoter region DNA fragments.** Two restriction digests of DNA from the *GAL1–10* intergenic region are shown, a *Hae*III-*Rsa*I double digest and a *Fok*I digest. Digests were electrophoresed under conditions (see "Experimental Procedures") designed to maximize the slow migration of DNA that contains internal bends and done either in the absence (*panel A*) or presence (*panel B*) of ethidium bromide (1 μg/ml). Standard DNA digests (ϕX-*Hae*III, pBR322-*Msp*I) were coelectrophoresed with the *GAL1–10* DNA to provide the calibration (*solid line*). The locations of the *GAL1–10* fragments labeled in the plots (*a–c, 1–3*) are identified in the map *above* the plots.

alies. Based on the slopes of the lines in these plots, one can estimate the average bending angle (39). For the 645-bp bend, this average angle is ~70° (Table I).

The bending models and the restriction digests predict two other strong bends, at sites around 500 bp on the *GAL1–10* promoter and around 500 bp on the *GAL80* promoter. Circular permutation analysis confirms both of these intrinsic bending sites (Fig. 5), at 536 bp on *GAL1–10* and at 551 bp on *GAL80*. Again, these migration anomalies are not observed in the presence of ethidium bromide (not shown). The estimated bending angles for these bends are ~50° for each (Table I).

These experimental results show fairly good agreement with the Goodsell and Dickerson bending model (37), which is based on nucleosome positioning data. For example, the experimentally determined bend centers and magnitudes of the *GAL1–10* 536- and 645-bp bends and the 551-bp bend of *GAL80* show

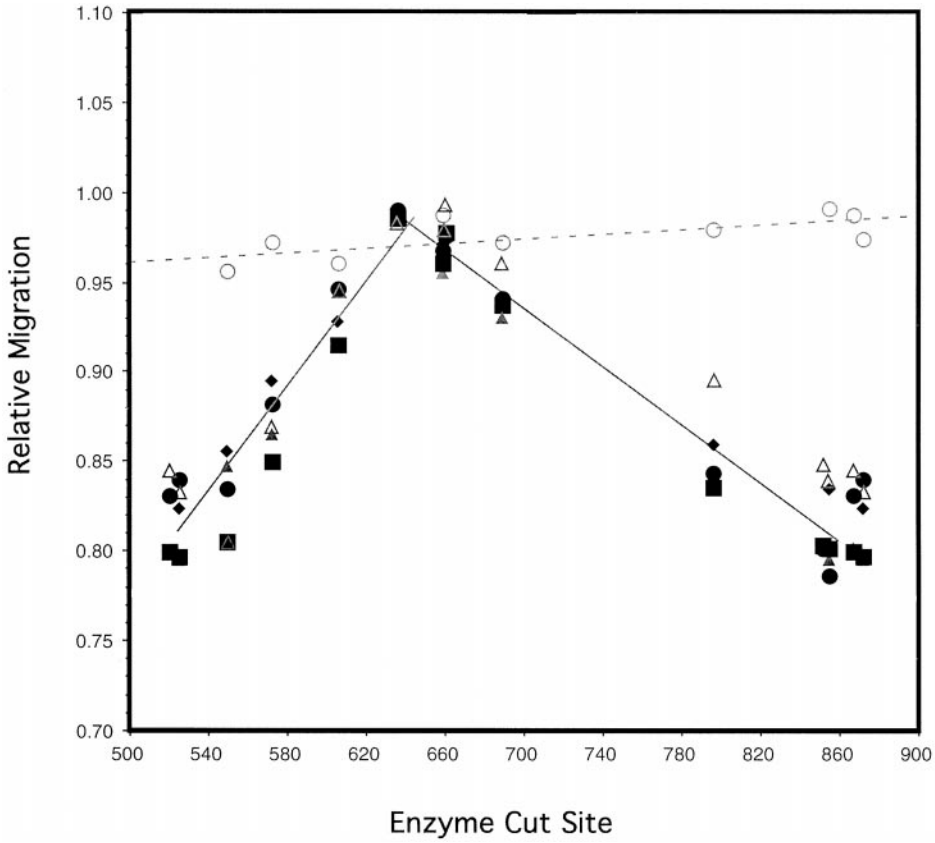

FIG. 4. **Circular permutation of the GAL1–10 550–896-bp fragment.** The results from five separate, independent electrophoretic runs are shown by the *closed symbols* (●, ■, ▲, ♦, △). The *lines* are best fits to the data from the five runs (average r^2 = 0.988). Relative migration is the ratio of the particular fragment mobility to the mobility that would be expected for the same size standard DNA fragment (See "Experimental Procedures"). Results from an electrophoretic analysis done in the presence of ethidium bromide are shown by the *open circles*.

TABLE I
Strong DNA bend locations

	Experimental		Predicted[a]	
	Bend center	Calculated bend angle	Bend center	Bend angle
	bp		*bp*	
GAL1	645	~70 °	651	86 °
GAL1	536	~50 °	529	50 °
GAL80	551	~50 °	560	50 °

[a] From LORDS analysis, Goodsell and Dickerson model (37).

excellent agreement with model predictions (Table I). Moreover, this model predicts a broad curvature above 900 bp on *GAL80* (well within the coding region), and we find evidence for a bend centered at 960 bp (not shown). Also, in our initial screen (gel migration anomalies), we did not detect evidence for any intrinsic promoter region bends besides those predicted by the Goodsell and Dickerson model. Thus, 300–500 bp on the *GAL1–10* promoter and 300–500 and 600–800 bp on the GAL80 promoter are bend-free.

The Goodsell and Dickerson model (Fig. 2*B*) also predicts two weaker bends just upstream of *GAL10* (at ~220 and ~280 bp) and a bend in the *GAL10* 5′ coding region (at ~130 bp). Another bending model, Brukner *et al.* (40), also predicts bends at ~130, ~190, and ~ 280 bp (not shown). Migration anomaly and circular permutation studies yield results that are consistent with the presence of bends at ~130 and ~200 bp (*cf.* fragments 32 *c* in Fig. 3*A* and data not shown), but there is a much greater variability in the mobility studies, and the circular permutation signals are much weaker for these bends than for the 536- and 645-bp bends. Thus, it is likely that there are intrinsic bends at ~130 and ~200 bp, but these bends are probably weaker than the *GAL1* proximal bends, as predicted (Table I). The close proximity of the three *GAL10*-proximal bends might also affect the strength of the bending signal from this region and definitely complicates circular permutation studies. We feel that these *GAL10*-proximal bends are not likely to be as important as the stronger bends upstream of *GAL1* and *GAL80* and therefore have not pursued their study. The bend centered at ~ 280 bp is predicted to be the weakest of the *GAL10*-proximal bends (Fig. 2*B*) and lies in a region with few restriction sites.

DISCUSSION

Using gel mobility and circular permutation analyses, we have detected fairly strong (≥50°) sites of intrinsic DNA bending in the promoters of the yeast *GAL1–10* structural genes and the *GAL80* regulatory gene. *In vivo*, these *GAL* promoters contain two distinct types of chromatin regions: constitutively non-nucleosomal hypersensitive regions in which the major promoter elements, the UAS_G, reside; and nucleosomal regions, where the TATA, Inr, and transcription start sites are found *(30)*. The single intrinsic DNA bend on the *GAL80* promoter lies in the non-nucleosomal region, between the UAS_{GAL80} and the more gene-proximal promoter elements (Fig. 6). The *GAL80*-specific UAS_{GAL80} activation sequence is the most upstream element on *GAL80* and is required for both basal and induced expression. The intrinsic DNA bend might help to bring this constitutively functioning promoter element closer to the gene or to the other promoter elements. Intrinsic bends on prokaryotic promoters often function in such an architectural role (9). There are no intrinsic bends in the nucleosomal regions of the *GAL80* promoter (α or *D*, Fig. 6).

In contrast, the intrinsic bends in the *GAL1–10* promoter are all found within the promoter nucleosomal regions. These nucleosomes (*A–C*, Fig. 6) cover the TATA and transcription start sites of *GAL1* and *GAL10* under inactive (noninducing) conditions, and their presence helps to implement gene repression in those carbon sources (*cf.* Refs. 25 and 30). The strongest bends lie at 536 and 645 bp within a nucleosome referred to as *B* (Fig. 6). *In vivo*, nucleosome B clearly has a strong locational preference, although it is not clear whether nucleosome B is abso-

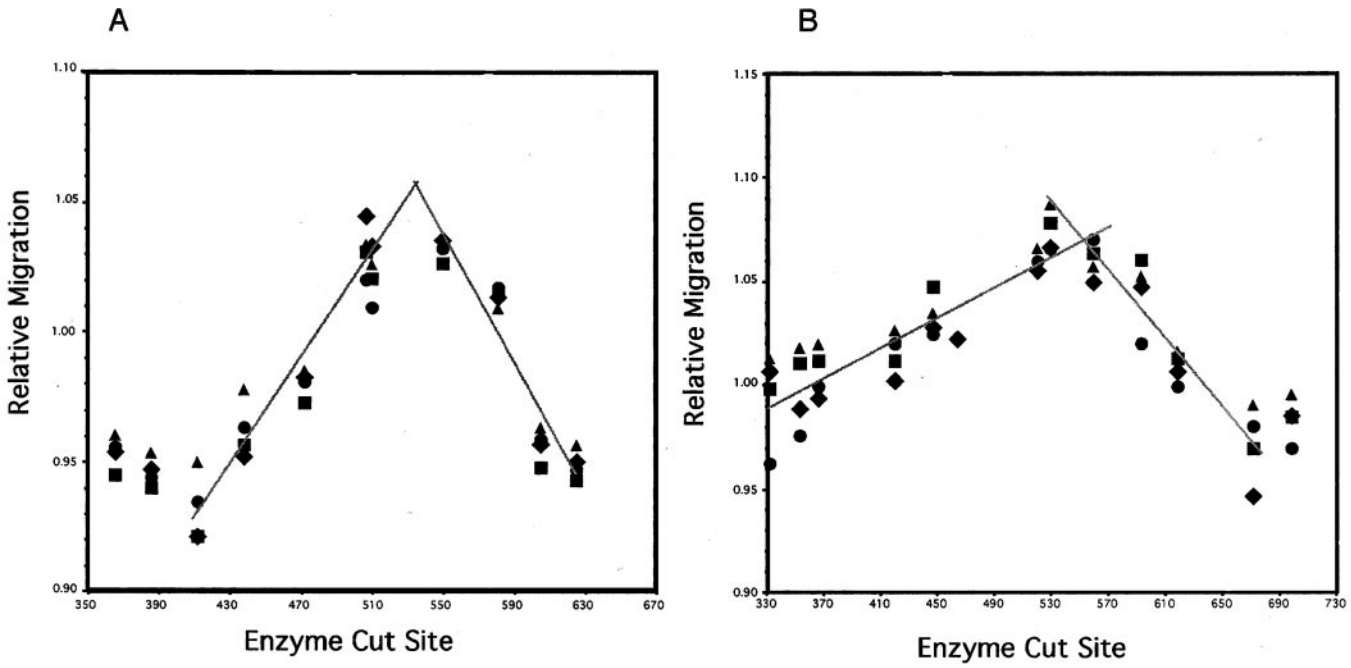

FIG. 5. **Circular permutation of the GAL1–10 366–606-bp fragment (*A*) and the GAL80 332–750-bp fragment (*B*).** The results from four separate, independent electrophoretic runs are shown by the *closed symbols* (●, ■, ▲, ♦). The lines are best fits to the data from the four runs (average $r^2 = 0.941$ (*A*) and 0.971 (*B*). Relative migration is the ratio of the particular fragment mobility to the mobility that would be expected for the same size standard DNA fragment.

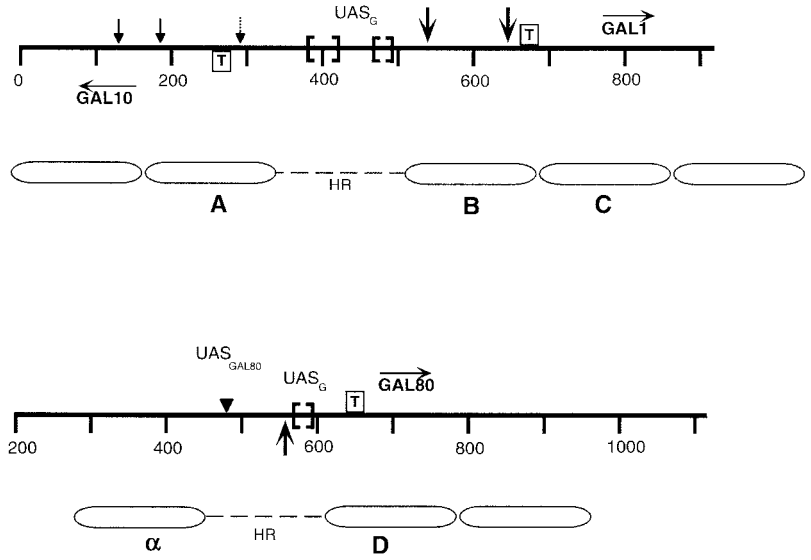

FIG. 6. **Location of intrinsic DNA bends.** Onto the *GAL1–10* and *GAL80* promoter region maps from Fig. 1 are superimposed the intrinsic bends determined from circular permutation, shown as *arrows above* (*GAL1–10*) or *below* (*GAL80*) the *thick lines*, and the promoter region chromatin structures, depicted *below* each DNA map. The *ovals* represent nucleosomes, labeled *A–C* on *GAL1–10* and α and *D* on *GAL80.* The *dashed lines* labeled *HR* locate the non-nucleosomal, hypersensitive regions found on each promoter. The *dotted arrow* reflects the fact that the bend at 280 bp is only a predicted bend.

lutely positioned (25). The dyad center of this nucleosome should lie around 595 bp (28), roughly midway between the two bending sites. Based on the nucleosome positions estimated by recent nuclease digestion studies (41, 42), the bend centers would lie within the terminal 20 bp or so on each end of a 147-bp core nucleosome B.

These two intrinsic DNA bends might help determine the location of nucleosome B in its preferred position. For example, it has been suggested that nucleosomes have a preference to locate more flexible DNA in their central region and that this can be a determinant of nucleosome positioning (43, 44). The preferred position of nucleosome B is consistent with this suggestion; it places the more rigid (intrinsically bent) DNA near the nucleosome termini, in regions where DNA is less constrained by nucleosome structure (45, 46) and locates the more flexible interbend DNA within the nucleosome. However, nucleosome B does not show positioning *in vitro* (47). Thus, these intrinsic bends are apparently not capable by themselves of imposing locational boundaries on nucleosome B. Other features that could also contribute to the *in vivo* positioning of nucleosome B have been discussed elsewhere (25). Despite the presence of these intrinsic bends, nucleosome B is stable, perhaps because the 110 bp of DNA between the two bending sites is close to the length of DNA (~120 bp) that is strongly associated with the core histones in the nucleosome (45, 46). Nevertheless, these intrinsic DNA bends might interfere enough with the normal wrapping of DNA on the nucleosome to cause B to be less stable than a nucleosome without such bends.

These two intrinsic bends may play their most important roles in the processes that are associated with the transcriptional activation of *GAL1*. 1) When *GAL1–10* expression is activated in galactose, the promoter nucleosomes (*A—C*, Fig. 6) appear to be completely removed (28, 48). The fact that the strongest bends on the *GAL1–10* intergenic region lie in nu-

cleosome B may reflect the central role of B in the nucleosome disruption process (for a review, see Ref. 25). For example, the bends could preferentially destabilize nucleosome B, either intrinsically (see above) or by attracting factors (see below), thus facilitating its complete disruption. The 645-bp bend also lies very near the nucleosome terminus that shows accessibility changes when histone H4 N termini are deleted or the acetylation sites are removed (41). These H4 mutations decrease *GAL1* induction levels by severalfold, indicating that the H4 tails normally play a role in *GAL1* activation. Perhaps that role involves the intrinsic bend.

2) It has been shown that placing an intrinsically bent DNA sequence between an upstream activation element and a TATA element will enhance transcription activation *in vivo* (20), and a bent sequence in phase with the TATA strongly enhances TBP-TATA binding (49). The center of the 645-bp bend lies 31 bp from the first TA step of the *GAL1* TATA, roughly three helical repeats of 10.5 bp, the solution repeat of DNA (50). Thus, the 645-bp bend could function to enhance TBP-TATA binding and *GAL1* expression, as observed in the model systems. The intrinsic bend and the bend induced by TBP would, if combined in phase, produce an ~150° bend.

3) The 645-bp bend may also recruit the yeast HMG analogues NHP 6A/6B, which are absolutely required for high-level *GAL1* induced expression *in vivo* (1). NHP6A displays an enhanced affinity for distorted DNA structures and bends DNA significantly upon binding to it (51, 52). Complete removal of nucleosome B (during gene induction) will expose both the 536- and 645-bp intrinsic bends to NHP6A, which could then bind to one or both of these bent sequences. Competition of NHP6A for these binding sites could even aid the nucleosome disruption process, at least thermodynamically. Bending induced by NHP6A binding should significantly shorten the distance between the UAS_G sequences and the TATA-bound TBP. Perhaps, more importantly, it has been shown *in vitro* that NHP6A stimulates polymerase II transcription by promoting the formation of an especially favorable TBP initiation complex (1). The bend at 645 bp would appear to be a suitable site from which NHP6A could promote the TBP complex assembly on *GAL1*. Both the TATA and UAS_G functions on *GAL1* depend on NHP6A/6B (1). Thus, the strong bends upstream of *GAL1* may function in nucleosome location in the inactive state and in gene activation during induction.

Acknowledgment—We thank Stefan Dieckmann for stimulating discussions.

REFERENCES

1. Paull, T., Carey, M., and Johnson, R. (1996) *Genes Dev.* **10,** 2769–2781
2. Dieckmann, S. (1987) *Nucleic Acids Mol. Biol.* **1**, 138–156
3. Crothers, D. M., Haran, T. E., and Nadeau, J. G. (1990) *J. Biol. Chem.* **265,** 7093–7096
4. Hagerman, P. J. (1990) *Annu. Rev. Biochem.* **59,** 755–781
5. Hagerman, P. (1992) *Biochim. Biophys. Acta* **1131,** 125–132
6. Wu, H. M., and Crothers, D. M. (1984) *Nature* **308,** 509–513
7. Dieckmann, S. (1989) *Electrophoresis* **10,** 354–359
8. Perez-Martin, J., Rojo, F., and de Lorenzo, V. (1994) *Microbiol. Rev.* **58,** 268–290
9. Perez-Martin, J., and de Lorenzo, V. (1997) *Annu. Rev. Microbiol.* **51,** 593–628
10. Schroth, G., Siino, J., Cooney C., Th'ng, J., Ho, P., and Bradbury, E. (1992) *J. Biol. Chem.* **267,** 9958–9964
11. Kawamoto, T., Makino, K., Orita, S., Nakata, A., and Kakunaga, T. (1989) *Nucleic Acids Res.* **17,** 523–537
12. Wada-Kiyama, Y., and Kiyama, R. (1994) *J. Biol. Chem.* **269,** 22238–22244
13. Nair, M. T. (1998) *FEBS Lett.* **422,** 94–98
14. Cress, W. D., and Nevins, J. R. (1996) *Mol. Cell. Biol.* **16,** 2119–2127
15. Falvo, J. V., Thanos, D., and Maniatis, T. (1995) *Cell* **83,** 1101–1111
16. Bustin, M., and Reeves, R. (1996) *Prog. Nucleic Acid Res. Mol. Biol.* **54,** 35–100
17. Nardulli, A. M., and Shapiro, D. J. (1992) *Mol. Cell. Biol.* **12,** 2037–2042
18. Kim, J., Klooster, S., and Shapiro, D. J. (1995) *J. Biol. Chem.* **270,** 1282–1288
19. Burley, S, and Roeder, R. (1996) *Annu. Rev. Biochem.* **65,** 769–799
20. Kim, J., de Haan, G., and Shapiro, D. J. (1996) *Biochem. Biophys. Res. Commun.* **226,** 638–644
21. Johnston, M. (1987) *Microbiol. Rev. 51,* 458–476
22. Johnston, M., and Carlson, M. (1992) in *The Molecular and Cellular Biology of the Yeast Saccharomyces: Gene Expression* (Jones E., Pringle, J., and Broach J., eds) Vol. II, pp. 193–281, Cold Spring Harbor Laboratory Press, Cold Spring Harbor, New York
23. Lohr, D., Venkov, P., and Zlatanova, J. (1995) *FASEB J.* **9,** 777–787
24. Reece, R. J., and Platt, A. (1997) *BioEssays* **19,** 1001–1010
25. Bash, R., and Lohr, D. (2000) *Prog. Nucleic Acid Res. Mol. Biol.* **65,** 197–259
26. Shimada, H., and Fukawawa, T. (1985) *Gene* **39,** 1–9
27. Sakurai, H., Ohishi, T., and Fukasawa, T. (1994) *Mol. Cell. Biol.* **14,** 6819–6828
28. Lohr, D. (1984) *Nucleic Acids Res.* **12,** 8457–8474
29. Lohr, D. (1993) *Proc. Natl. Acad. Sci. U. S. A.* **90,** 10628–10632
30. Lohr, D. (1997) *J. Biol. Chem.* **272,** 26795–26798
31. Lohr, D., and Hopper, J. (1985) *Nucleic Acids Res.* **13,** 8409–8423
32. Birnboim, H. C. (1983) *Methods Enzymol.* **100,** 243–255
33. Maxam, A. M., and Gilbert, W. (1980) *Methods Enzymol.* **65,** 499–560
34. Dieckmann, S., and Lilley, D. M. J. (1987) *Nucleic Acids Res.* **15,** 5765–5774
35. Sambrook, J., Fritsch, E. F., Maniatis, T. (1989) in *Molecular Cloning*, Ed. 2, pp. 1, 68–86, Cold Spring Harbor Laboratory Press, Cold Spring Harbor, New York
36. Bolshoy, P., McNamara, P., Harrington, R., and Trifonov, E. (1991) *Proc. Natl. Acad. Sci. U. S. A.* **88,** 2313–2316
37. Goodsell, D., and Dickerson, R. (1994) *Nucleic Acids Res.* **22,** 5497–5503
38. Ulyanov, N., and James, T. (1995) *Methods Enzymol.* **261,** 90–120
39. Thompson, J. F., and Landy, A. (1988) *Nucleic Acids Res.* **16,** 9687–9705
40. Brukner, I., Sanchez, R., Suck, D., and Pongor, S. (1995) *EMBO J.* **14,** 1812–1818
41. Fisher-Adams, G., and Grunstein, M. (1995) *EMBO J.* **14,** 1468–1477
42. Reagan, M., and Majors, J. (1998) *Mol. Gen. Genet.* **259,** 142–149
43. Fitzgerald, D., Dryden, G., Bronson, E., Williams, J., and Anderson, J. (1994) *J. Biol. Chem.* **269,** 21303–21314
44. Widlund, H., Kuduvalli, P., Bengtsson, M., Hui, C., Tullius, T., and Kubista, M. (1999) *J. Biol. Chem.* **274,** 31847–31852
45. Van Holde, K. (1988) *Chromatin,* pp. 247–251, Springer-Verlag, New York
46. Luger, K., Mäder, A., Richmond, R., Sargent, D., and Richmond, T. (1997) *Nature* **389,** 251–260
47. Rainbow, M., Lopez, J., and Lohr, D. (1989) *Biochemistry* **28,** 7486–7490
48. Lohr, D., and Lopez, J. (1995) *J. Biol. Chem.* **270,** 27671–27678
49. Parvin, J. A., McCormick, R. J., Sharp, P. A., and Fisher. D. E. (1995) *Nature* **373,** 724–727
50. Peck, L. J., and Wang, J. C. (1981) *Nature* **292,** 375–378
51. Paull, T., and Johnson, R. (1995) *J. Biol. Chem.* **270,** 8744–8875
52. Yen, Y-M., Wong, B., and Johnson, R. C. (1998) *J. Biolem. Chem.* **273,** 4424–4435